J. Fluid Mech. (2016), *vol.* 807, R1, doi:10.1017/jfm.2016.605



JFM RAPIDS
journals.cambridge.org/rapids

Scaling laws for segregation forces in dense sheared granular flows

François Guillard[1,2,†], **Yoël Forterre**[1] **and Olivier Pouliquen**[1]

[1]Aix-Marseille Université, CNRS, IUSTI UMR 7343, 13453 Marseille, France
[2]Particles and Grains Laboratory, School of Civil Engineering, University of Sydney, NSW 2006, Australia

(Received 19 July 2016; revised 9 September 2016; accepted 14 September 2016; first published online 18 October 2016)

In order to better understand the mechanism governing segregation in dense granular flows, the force experienced by a large particle embedded in a granular flow made of small particles is studied using discrete numerical simulations. Accurate force measurements have been obtained in a large range of flow parameters by trapping the large particle in a harmonic potential well to mimic an optical tweezer. Results show that positive or negative segregation lift forces (perpendicular to the shear) exist depending on the stress inhomogeneity. An empirical expression of the segregation force is proposed as a sum of a term proportional to the gradient of pressure and a term proportional to the gradient of shear stress, which both depend on the local friction and particle size ratio.

Key words: granular media, granular mixing

1. Introduction

A rich phenomenology is observed owing to segregation occurring in flows of polydispersed granular material. When flowing, large and small particles have a tendency to migrate in different regions, giving rise to complex patterns such as stripes and bands in rotating drums (Hill, Caprihan & Kakalios 1997; Aranson & Tsimring 2006), levees and fingers at the front of avalanches (Pouliquen, Delour & Savage 1997; Félix & Thomas 2004*b*; Woodhouse *et al.* 2012), and channels in silo flows (Fan & Hill 2011). This tendency to segregate is a major source of problems in many industrial applications involving mixing processes, and is at the origin of geomorphological patterns observed in deposits of rock avalanches, landslides or pyroclastic flows (Kokelaar *et al.* 2014).

A lot of effort has been devoted to the development of a theoretical framework able to describe the flow of polydispersed material. In the case of dilute collisional

† Email address for correspondence: francois.guillard@sydney.edu.au

© Cambridge University Press 2016

https://doi.org/10.1017/jfm.2016.605 Published online by Cambridge University Press

granular flows, segregation can be predicted within the framework of the kinetic theory for various concentrations of the different species (Jenkins & Mancini 1989; Brey, Ruiz-Montero & Moreno 2005). This approach, valid in the dilute regime, fails to predict qualitatively the direction of segregation in the dense regime. Savage & Lun (1988), in a pioneering work, proposed a kinetic sieving mechanism to explain segregation in the dense regime for flows down an inclined plane. The picture is the following: during the flow, the fluctuating motion of the particles creates holes, and large grains can fall only in large holes, while small grains can fall in both small and large holes. This asymmetry in the exchange of grains between layers explains the rising of large particles at the free surface of the flow. This kinetic sieving process has been further developed in the context of mixture theory, where the partial stress carried by the different constituents of the mixture depends on their sizes, leading to segregation fluxes. Flows down inclined planes (Marks, Rognon & Einav 2011), segregation at the front of avalanches (Thornton & Gray 2008; Woodhouse *et al.* 2012), and segregation observed in rotating drums (Schlick *et al.* 2015) or in silos (Fan & Hill 2015) have been successfully modelled using this framework. However, the expression for the segregation flux remains largely empirical, and would benefit from a better understanding of the underlying physics controlling the segregation phenomenon. Moreover, the kinetic sieving mechanism seems to be insufficient to account for some experimental observations. Heavy enough particles can sink instead of rising up during the flow on inclined plane or in rotating drum (Thomas 2000; Félix & Thomas 2004*a*), showing that gravity forces can overcome segregation. This result suggests that a dynamic picture in term of forces may be more appropriate to describe the segregation phenomenon. However, what controls this force is not clear. For example, when comparing segregation on an inclined plane and in a silo, large particles go to low-shear regions in flows down inclined planes, whereas they migrate towards regions of high shear in dense flows in a silo (Fan & Hill 2011).

The objective of the present work is to precisely investigate the segregation force on a single coarse particle in a bath of small particles using two-dimensional (2D) discrete element simulations, in order to understand under which conditions segregation occurs and what are the relevant control parameters. The configuration studied in our simulations and the method used to measure the segregation force is presented in § 2. The results and scaling laws deduced from simulations in different shear flow configurations are shown in § 3. Discussion of the main results and conclusion are given in § 4.

2. Simulations and methods

The configuration of interest is sketched in figure 1(*a*). To be able to perform a large number of simulations changing a wide range of control parameters, we restrict our study to a 2D granular medium made of disks that is periodic in the x direction. The medium is made of disks of mean diameter $d = 1.5$ mm with a slight polydispersity of 20 % and density $\rho_p = 2500$ kg m^{-3}. The medium is sheared between two rigid rough plates made of a random layer of particles glued together (figure 1*a*). The simulations are made using the open source discrete element software LIGGGHTS (Kloss *et al.* 2012). The code is based on a molecular dynamics method for soft, inelastic, frictional spheres. The interaction forces between the particles are described in figure 1(*b*) and correspond to a Hooke contact law with friction and dissipation. The normal force between two particles in contact is modelled by a spring-dashpot system of stiffness $k_n = 81.10^4$ N m^{-1}, viscosity $\gamma_n = 12$ kg s^{-1}, whereas the tangential force

https://doi.org/10.1017/jfm.2016.605 Published online by Cambridge University Press

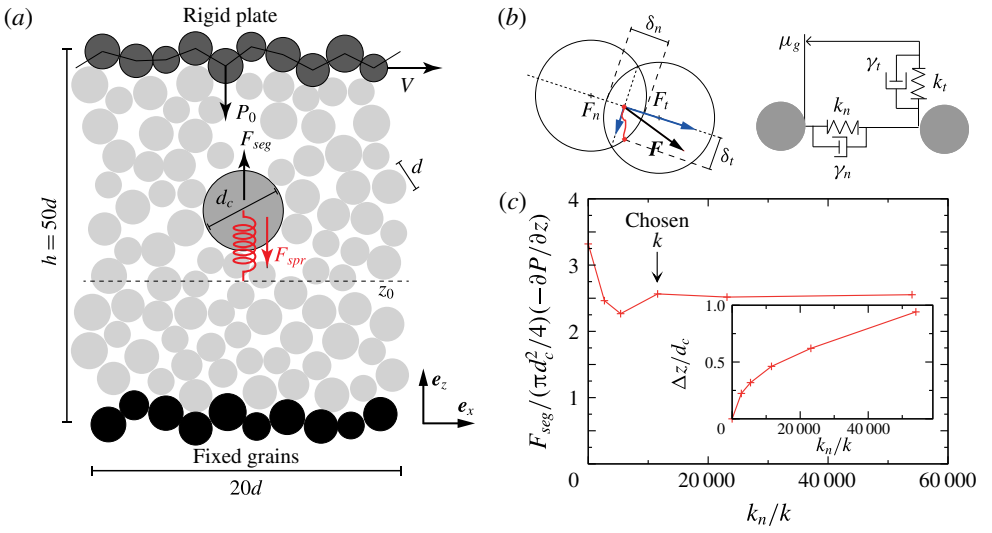


FIGURE 1. (*a*) Sketch of the simulated configuration. The bottom plate is fixed; the top plate is rigid and moves at a velocity V and is submitted to a pressure P_0. The coarse particle of diameter d_c is vertically confined in a harmonic potential of stiffness k. (*b*) Mechanical model for the contact forces between particles in the simulation. The coefficients used are $k_n = 81.10^4$ N m^{-1}, $k_t = 86.10^4$ N m^{-1}, $\gamma_n = \gamma_t = 12$ kg s^{-1}, $\mu_g = 0.5$. (*c*) Segregation force F_{seg} scaled by buoyancy measured for different spring stiffnesses k scaled by particle normal contact stiffness k_n. The arrow indicates the spring stiffness k used in the study. Simulation for $P_0 = 1900$ Pa, $\mu = |\tau|/P = 0.39$, $\boldsymbol{g} = -7.5$ m s$^{-2}\boldsymbol{e}_z$, $d_c = 4\,d$. Inset: standard deviation of the vertical position of the coarse particle scaled by its diameter function of the scaled spring stiffness.

is a Coulomb sliding block with friction coefficient $\mu_g = 0.5$ coupled with a spring dashpot (stiffness $k_t = 86.10^4$ N m^{-1} and viscosity $\gamma_t = \gamma_n$). The granular medium is confined under a pressure P_0 by applying a constant downward force on each particle of the top plate. The typical range of pressure is 500 Pa $< P_0 <$ 9500 Pa. The shear is prescribed by imposing a velocity V at the top plate in the range 0.4 m s$^{-1} < V <$ 7.5 m s^{-1}. In addition to the boundary conditions imposed by the top rigid plate, a body gravity field might be applied to the granular medium either in the vertical $-z$ direction, in the horizontal x direction or in any inclined directions $\boldsymbol{g} = g_x\boldsymbol{e}_x - g_z\boldsymbol{e}_z$. Typical levels of gravity investigated in this study are in the range $0 < g < 7.5$ m s^{-2}.

In the absence of gravity the system is symmetric and the stresses are homogeneous along the z direction (figure 2*d*). As a result, when the medium is sheared the measured velocity profile is linear (figure 2*c*), defining a constant shear rate $\dot{\gamma} = V/h$. In the following we restrict our study to the dense flow regime for which the inertial number $I = \dot{\gamma}d/\sqrt{P_0/\rho_p}$ is in the range $4 \times 10^{-3} < I < 0.25$ (corresponding to volume fraction $\phi > 0.74$). The shape of the constitutive laws for the effective friction coefficient $\mu(I)$ and volume fraction $\phi(I)$ are shown in figure 2(*a*,*b*). In the quasi-static regime when $I \to 0$, the friction coefficient is $\mu_c = 0.28$ and the critical volume fraction is $\phi_c = 0.82$, consistent with previous studies on 2D frictional discs (Da Cruz *et al.* 2005). As soon as a vertical gravity (respectively a horizontal gravity) is applied, the stress distribution is no longer uniform along z, and a gradient of pressure (respectively a gradient of shear stress) develops, leading to an asymmetric

https://doi.org/10.1017/jfm.2016.605 Published online by Cambridge University Press

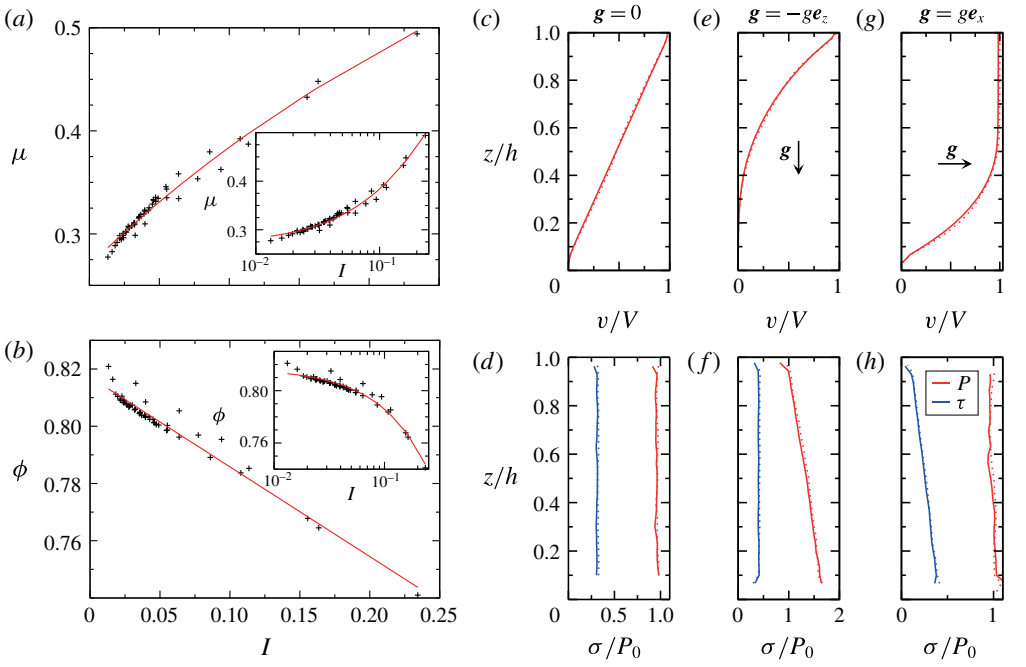


FIGURE 2. Friction coefficient $\mu = |\tau|/P$ (a) and volume fraction ϕ (b) as a function of the inertial number I for homogeneous plane shear ($\boldsymbol{g} = \boldsymbol{0}$). Average velocity profiles (c,e,g) and corresponding stress profiles (d,f,h) for $\boldsymbol{g} = \boldsymbol{0}$ (c,d), $\boldsymbol{g} = -7.5$ m s$^{-2}\boldsymbol{e}_z$ (e,f) and $\boldsymbol{g} = 7.5$ m s$^{-2}\boldsymbol{e}_x$ (g,h). The top plate velocity is $V = 2.5$ m s^{-1} and the confining pressure is $P_0 = 1600$ Pa $(c$–$f)$ or $P_0 = 4500$ Pa (g,h). Dotted lines are measured with the intruder, at $\bar{z}_m/h = 0.5$ (c,d), $\bar{z}_m/h = 0.76$ (e,f), $\bar{z}_m/h = 0.27$ (g,h).

velocity profile, as shown in figure 2$(e$–$h)$. By controlling the direction of gravity, one can thus switch from a configuration where asymmetry comes from a pressure gradient to a configuration where asymmetry comes from a shear stress gradient like in silo flows.

To study segregation in this configuration, a test particle of diameter d_c and same density as the bulk particles is introduced at different positions in the layer (figure 1a). In most simulations, the test particle diameter d_c is larger than the diameter d of the bulk particles. To accurately measure the force experienced by the test particle, we mimic the existence of a harmonic optical trap in the z direction for the test particle only. In addition to the gravity and to the contact forces exerted by the other particles, a force $F_{spr} = -k \times (z - z_0)\boldsymbol{e}_z$ is imposed to the large particle, where z is its vertical position and z_0 a reference position. The coarse particle is thus attached with a spring of stiffness k to the vertical position z_0, but is free to move horizontally with the flow. When the stationary regime is reached, the coarse particle flows with the bulk but remains on average at a fixed altitude z_m. This equilibrium position in the vertical direction results from the balance between three forces: the weight of the test particle $-m_c g_z$, where $m_c = \rho_g \pi d_c^2/4$ is the mass of the test particle, the spring force $-k(z_m - z_0)$ and the segregation force F_{seg}, defined as the sum of the vertical contributions of the contact forces exerted by the small particles on the test particle. The segregation force F_{seg} can thus be estimated either from the shift in the vertical position $F_{seg} = k(\bar{z}_m - z_0) + m_c g_z$, $\bar{z}_m$ being the time-averaged vertical position of the

https://doi.org/10.1017/jfm.2016.605 Published online by Cambridge University Press

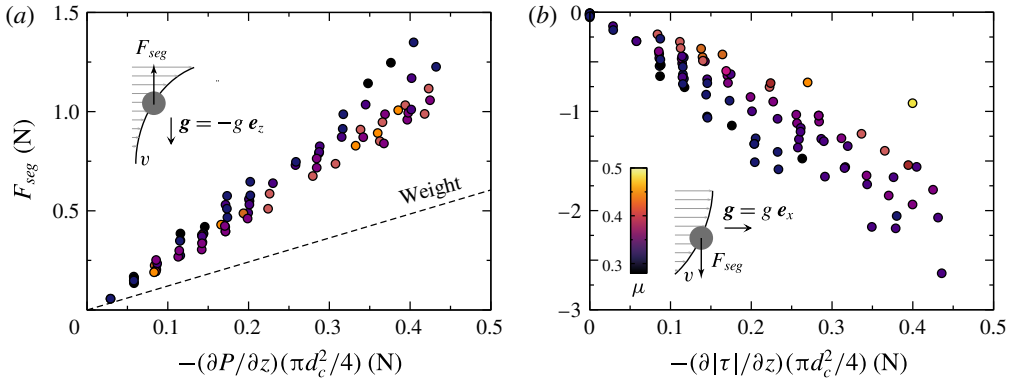


FIGURE 3. Segregation force as a function of the buoyancy $-(\pi {d_c}^2/4)(\partial P/\partial z)$ for simulations with vertical gravity $\boldsymbol{g} = -g\,\boldsymbol{e}_z$ (*a*) and as a function of $-(\pi {d_c}^2/4)(\partial|\tau|/\partial z)$ for simulations with horizontal gravity $\boldsymbol{g} = g\,\boldsymbol{e}_x$ (*b*). Dotted lines correspond to the weight of the coarse particle ($d_c = 4\,d$). Symbols are coloured by the local friction coefficient $\mu = |\tau|/P$. Uncertainty of the average forces are of the order of the point size.

test particle, or directly by computing the time average of the sum of the contact forces experienced by the coarse particle. We have checked that both methods give the same results. We have also checked that the measure of F_{seg} is independent of the external spring stiffness k, as long as it is much smaller than the grain stiffness (figure 1*c*). Note that the fluctuations of the vertical position of the trapped particle increase with k_n/k, but have no effect on the measured segregation force (figure 1*c*, inset). In the following we choose $k = 70$ N m^{-1}.

Notably, for some combination of P_0 and g, non-flowing zones where the local friction coefficient $\mu = |\tau|/P$ is below the minimal friction coefficient μ_c can appear, either at the bottom of the sample in the case $\boldsymbol{g} = -g\boldsymbol{e}_z$ or at the top in the case $\boldsymbol{g} = g\boldsymbol{e}_x$. This effect limits the range of g that can be explored, and simulations where the coarse particle position z_m ends up in one of these pseudo-static zones, where $\mu < \mu_c$, have been discarded.

3. Results

A large number of simulations have been carried out to investigate how the segregation force evolves depending on the flow conditions. We first set the size of the coarse particle equal to $d_c = 4d$. A key control parameter in the segregation problem is the gravity imposed to the system. In absence of gravity, no mean lift force is measured on the large particle, as expected from symmetry argument. As soon as gravity is switched on, the up/down symmetry is broken and a segregation force is measured. As a first step in our analysis, the two cases corresponding, respectively, to a vertical and a horizontal gravity are studied independently and results are presented in figure 3(*a*,*b*), respectively.

Let us first consider the case with a vertical gravity, $\boldsymbol{g} = -g\,\boldsymbol{e}_z$. The force balance implies that a gradient of vertical normal stress (called pressure below for sake of simplicity) $\partial P/\partial z$ exists, the shear stress τ being constant across the layer (figure 2*f*). In figure 3(*a*) the segregation force F_{seg} is plotted as a function of the two-dimensional buoyancy force $-(\pi {d_c}^2/4)(\partial P/\partial z)$, with $(\partial P/\partial z)$ being measured far from the coarse particle but at the vertical level corresponding to its steady mean position.

https://doi.org/10.1017/jfm.2016.605 Published online by Cambridge University Press

Dimensionally, buoyancy is the only force one can construct based on the stress gradient. Moreover, it has been shown to be the relevant scaling for the lift force experienced by an object moving in a static granular medium (Guillard, Forterre & Pouliquen 2014). The different points in figure 3(*a*) are obtained for different levels of gravity g, different confining pressures P_0, different shear velocities V and different mean positions z_m in the layer. The first observation is that the segregation force is positive and equal to approximately twice the weight of the coarse particle, meaning that the coarse particle in the same configuration, but without the spring, would rise up to the top, i.e. in the direction opposite to the pressure gradient. The second result is that the segregation force follows an approximately linear variation with the buoyancy force. However, this scaling does not entirely capture the variation, as a significant scatter exists, a point that will be discussed later.

We now turn to the case of a horizontal gravity, $\boldsymbol{g} = g\,\boldsymbol{e}_x$. In this case the force balance implies that a gradient of shear stress $\partial|\tau|/\partial z$ exists, the normal stress P being constant across the layer. In figure 3(*b*) the segregation forces measured for different g, P_0, V and position z_0 are plotted versus $-(\pi {d_c}^2/4)(\partial|\tau|/\partial z)$, by analogy with the buoyancy force. In this case the measured segregation force is negative, meaning that the coarse particle in the presence of a shear stress gradient has a tendency to sink in the direction of the gradient, in opposition to the previous case. Notice that the relevant control parameter is the gradient of the modulus of the shear stress, as changing the sign of the gravity from $\boldsymbol{g} = g\,\boldsymbol{e}_x$ to $\boldsymbol{g} = -g\,\boldsymbol{e}_x$ and velocity from $V_0\,\boldsymbol{e}_x$ to $-V_0\,\boldsymbol{e}_x$ does not change the segregation force while changing the sign of τ and $\partial\tau/\partial z$. Figure 3(*b*) shows that the segregation force in this case also varies linearly with the buoyancy-like force, although again the scaling is not perfect and does not capture the entire behaviour.

A more careful analysis of figure 3 shows that data are ordered according to the friction coefficient $\mu = |\tau|/P$ indicated by the colour of the symbols. This suggests that the segregation force might scale with the stress gradients times a function of the friction coefficient. To test this hypothesis, we plot in figure 4 the ratio of the segregation force over the buoyancy-like force for the vertical and horizontal gravity, as a function of the friction coefficient. All data obtained for different flow parameters collapse on two main curves for the cases of vertical and horizontal gravity, suggesting the following expressions for the segregation force:

$$F_{seg} = -\mathcal{F}(\mu)\,\frac{\pi {d_c}^2}{4}\frac{\partial P}{\partial z} \quad \text{for } \boldsymbol{g} = -g\,\boldsymbol{e}_z, \tag{3.1}$$

$$F_{seg} = -\mathcal{G}(\mu)\,\frac{\pi {d_c}^2}{4}\frac{\partial |\tau|}{\partial z} \quad \text{for } \boldsymbol{g} = g\,\boldsymbol{e}_x. \tag{3.2}$$

$\mathcal{F}(\mu)$ and $\mathcal{G}(\mu)$ are functions of the local friction coefficient $\mu = |\tau|/P$ and can be empirically fitted from figure 4 by $\mathcal{F}(\mu) = 2.4 + 0.73\exp(-(\mu - \mu_c)/0.051)$ and $\mathcal{G}(\mu) = -(2 + 5.5\exp(-(\mu - \mu_c)/0.076))$.

These expressions thus provide the scaling of the segregation force for the two distinct cases of either a vertical or a horizontal gravity. To generalize this result, we now consider an inclined gravity, when both a pressure gradient and a shear stress gradient exist. A linear expansion of the segregation force as a function of the stress gradients suggests that the segregation force might simply be the sum of the two contributions given by (3.1) and (3.2). To test this idea, simulations have been carried out for gravity at different inclinations θ from vertical ($0 < \theta < 90°$) and for two levels of gravity (circles and squares in figure 5). For each run, the measured segregation

https://doi.org/10.1017/jfm.2016.605 Published online by Cambridge University Press

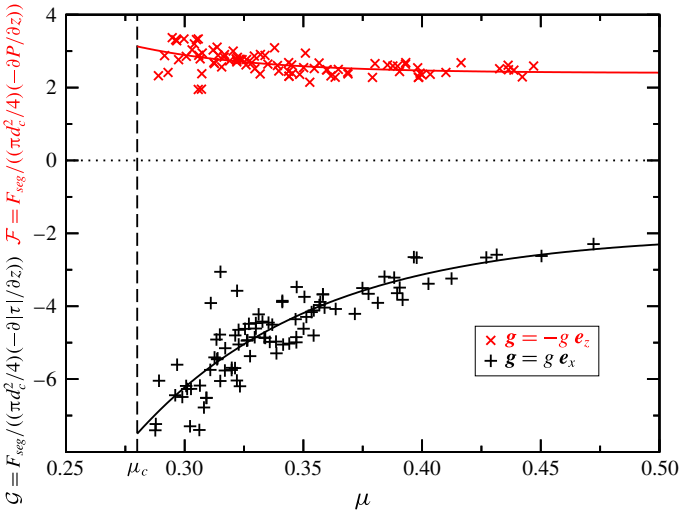


FIGURE 4. Segregation force F_{seg} scaled by the buoyancy-like forces (see (3.1) and (3.2)) as a function of the local friction coefficient μ for both the vertical ($\mathcal{F}$, red) and horizontal ($\mathcal{G}$, black) gravity cases. Lines are fits of the data by exponential functions: $\mathcal{F}(\mu) = 2.4 + 0.73\exp(-(\mu - \mu_c)/0.051)$, and $\mathcal{G}(\mu) = -(2 + 5.5\exp(-(\mu - \mu_c)/0.076))$. Data obtained for $d_c = 4\,d$.

force F_{seg} experienced by the coarse particle is compared to the prediction F_{seg}^{th} given by the sum of the two expressions (3.1) and (3.2), in which P, $|\tau|$, $\partial P/\partial z$ and $\partial|\tau|/\partial z$ are measured far from the coarse particle but at the same vertical position. Figure 5 shows that the experimental points nicely collapse on the $F_{seg} = F_{seg}^{th}$ line, showing the relevance of the additivity assumption. In this figure, we also report simulations made for flows down inclined planes (triangles), which correspond to the configuration of figure 1(*a*) in which the top plate has been removed and $P_0 = 0$, $g = 9.81$ m s^{-2}. In this case, the ratio of shear to normal stress (μ) is constant across the layer, but both a pressure and a shear stress gradient exist. Although a limited range of inclinations gives rise to a steady flow, the data collapse on the same line as before, except at the highest inclination $\theta = 30°$, where the system enters a more dilute and collisional regime (see inset of figure 5). All together, these results show that the segregation force is correctly captured by the sum of the two contributions given by (3.1) and (3.2).

So far, all data have been obtained for a coarse particle diameter $d_c = 4\,d$. Figure 6 shows how the segregation force varies as function of the size ratio d_c/d for a wide range of test particle diameter $0.5\,d < d_c < 10\,d$ and vertical (red dots) or horizontal (black dots) gravity. When the diameter of the test particle is equal to the mean diameter of the bulk particle, $d_c/d = 1$, no segregation effect is expected. This implies a segregation force equal to the weight of the particle in the case of vertical gravity (that is $F_{seg} = -(1/\phi)(\pi {d_c}^2/4)(\partial P/\partial z)$, since hydrostatic equilibrium implies $(\partial P/\partial z) = -\rho_p \phi g$, with $\phi \sim 0.8$ the volume fraction of grains) and $F_{seg} = 0$ in the case of horizontal gravity. Our direct measurement of the segregation force in figure 6 is coherent with this picture, with $\mathcal{F} = 1/\phi$ and $\mathcal{G} = 0$ for $d_c \approx 1.06\,d$, the uncertainty coming from the polydispersity of our medium. When the diameter of the test particle increases, the amplitude of the segregation force induced by a pressure gradient or a

https://doi.org/10.1017/jfm.2016.605 Published online by Cambridge University Press

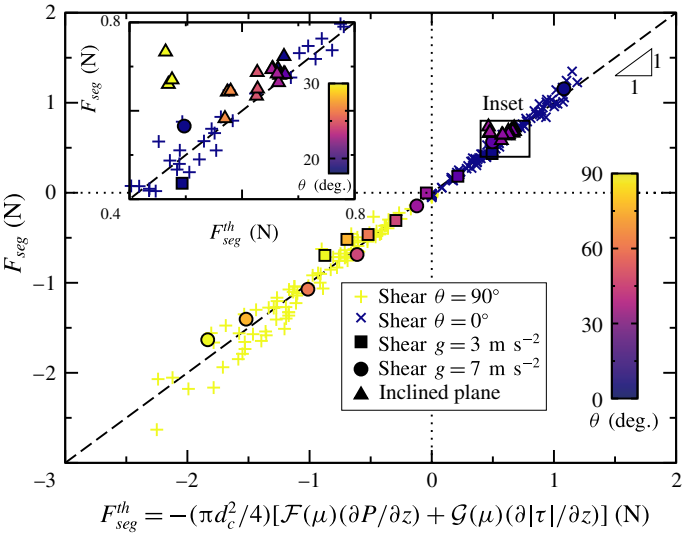


FIGURE 5. Measured segregation force F_{seg} as a function as the predicted force $F_{seg} = F^{th}_{seg}$ based on the sum of the empirical vertical and horizontal stress gradient contribution given by (3.1) and (3.2). (■ and ●): shear cell configuration with inclined gravity; (▲): inclined plane configuration. The data from figure 4 are also indicated (× and +). Colours of the symbols indicate the inclination angle θ of the gravity from $-z$. Inset: close up around the data corresponding to the inclined plane simulations. Data obtained for $d_c = 4\,d$.

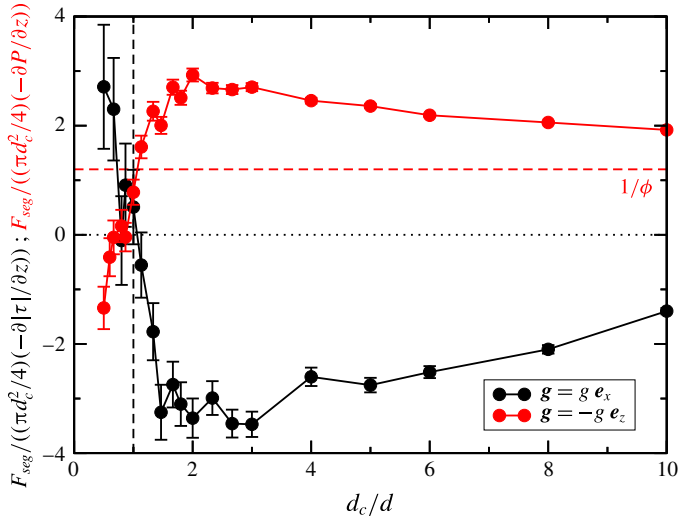


FIGURE 6. Scaled segregation force as a function of the ratio of particle size d_c/d for the two gravity directions. $V = 7.5$ m s^{-1}, $g = 3$ m s^{-2}, μ in between 0.4 and 0.42.

shear stress gradient rapidly increases, reaching a maximum at approximately $d_c/d = 2$, before slowly decreasing at large size ratio. No measurements are given for $d_c > 10\,d$, as in this case the system becomes strongly inhomogeneous on the size of the test particle. The case of a small test particle $d_c/d < 1$ is also of interest. The segregation

https://doi.org/10.1017/jfm.2016.605 Published online by Cambridge University Press

force decreases and becomes less than the weight (respectively larger than zero) for the case of a vertical (respectively horizontal) gravity, thus reversing the segregation direction. Notably, the evolution of the segregation force close to $d_c/d = 1$ is very steep, showing that a slight difference in size has dramatic effects in terms of the segregation phenomenon. To conclude, we can thus propose the following empirical expression for the segregation force as a function of the stress gradients:

$$F_{seg} = -\pi \frac{d_c^2}{4} \left(\mathcal{F}(\mu, d_c/d) \frac{\partial P}{\partial z} + \mathcal{G}(\mu, d_c/d) \frac{\partial |\tau|}{\partial z} \right), \tag{3.3}$$

with $\mathcal{F}(\mu,\ d_c/d)$ and $\mathcal{G}(\mu,\ d_c/d)$ being two empirical functions of the friction coefficient $\mu = |\tau|/P$ and of the size ratio d_c/d satisfying $\mathcal{F}(\mu,\ 1) = 1/\phi(\mu)$ and $\mathcal{G}(\mu,\ 1) = 0$. The volume fraction $\phi(\mu)$ decreases with μ due to the increase of collisions, and is given in figure 2(*b*) or in Da Cruz *et al.* (2005). The dependence of $\mathcal{F}$ and $\mathcal{G}$ with μ and d_c/d is given in figures 4 and 6.

4. Discussions

By imposing a harmonic vertical trap in a simple shear flow, we have been able to precisely measure the lift force experienced by one large particle flowing in a bath of small particles in a wide range of flow parameters and for different stress distributions. We have shown that a segregation force develops, which strongly depends on the size ratio and on the stress inhomogeneities existing in the material. An empirical scaling law has been proposed for the segregation force as a sum of a term proportional to the gradient of pressure and a term proportional to the gradient of shear stress: large particles have a tendency to migrate towards regions of low pressure and/or regions of high shear stress.

The evidence of two contributions of opposite sign in the segregation force provides a simple unified framework to describe the different observations made in the literature. First, for dense flows in silos, it has been reported that large particles migrate towards the walls, i.e. towards regions of high shear rate (Fan & Hill 2011). Such observations can be understood in the framework proposed in this study: large grains simply migrate towards the region of high shear stress, the pressure being uniform. This interpretation in terms of the shear stress gradients contrasts with the model proposed by Fan & Hill (2015), which is based on a kinetic contribution to the stress. However, kinetic stresses are supposed to vanish in the limit of quasi-static flows, whereas our simulations show that a shear-stress-induced segregation force still exists in this limit. A second configuration that has been extensively studied is the free surface flow of bidispersed material on inclined planes. The large particles are found to rise up at the free surface, i.e. towards regions of low shear rate. In terms of stress inhomogeneities, both pressure and shear stress gradients are present in this configuration, but at the low inclinations where steady dense flows are observed, the pressure gradient always dominates, leading to an upward segregation, as observed. Interestingly, experiments of granular flows down inclines using spheres have shown that the segregation may be reversed for large size ratio ($d_c/d > 6$) (Félix & Thomas 2004*a*). Our result does not show a change of sign of the segregation force when increasing size ratio, but the existence of two antagonistic forces, one pushing towards the region of high shear stress (at the bottom of the inclined plane), the other towards the low-pressure region at the free surface, may give rise to a complex dependence with inclination and size ratio. The qualitative agreement between our

https://doi.org/10.1017/jfm.2016.605 Published online by Cambridge University Press

2D simulations and these observations in 3D systems suggests that the scaling for the segregation force evidenced in our study remains in 3D. However, for a more quantitative comparison, it would be interesting to perform a similar numerical study using 3D discrete element methods.

Beyond the qualitative prediction of the direction of segregation in different configurations, the empirical formula proposed in this study for the segregation force might be useful to predict segregation fluxes in mixtures of grains of different sizes. Coupling the expression for the segregation force with the knowledge of the drag force experienced when one single particle moves relatively to the others, as studied in Tripathi & Khakhar (2011), should in principle give rise to a prediction of the segregation velocity when the particle is free to move, and thus to the prediction of the segregation flux in the limit of vanishing concentration of large particles. However, the case of mixtures of high concentration is more complex, as interactions between coarse particles start to play a major role, as discussed by several authors in the context of the mixture theory (Thornton & Gray 2008; Marks *et al.* 2011; Woodhouse *et al.* 2012; Schlick *et al.* 2015).

Finally, understanding the physical origin of the segregation force and scalings put in evidence in our study remains a real challenge. In the presence of pressure gradients (vertical gravity) a simple argument based on the frictional nature of the granular rheology might be relevant. The argument is the following: the net segregation force is the sum of the forces experienced by the top and the bottom parts of the coarse particle. Both forces are opposite with same magnitude when the pressure is uniform but, as they scale with the mean pressure level (since the rheology is frictional), the force on the bottom becomes larger in the presence of a pressure gradient, inducing a net upward force (Guillard *et al.* 2014). The contribution of the shear stress gradient to the segregation force is more difficult to understand, and we have not been able to find a simple qualitative argument able to explain our findings. But considering the richness and complexity of the problem of the forces on a particle in a sheared Newtonian fluid (Guazzelli & Morris 2011), it is not surprising to find non-trivial effects in the highly non-Newtonian case of a flowing granular medium. Studying the force on a sphere using a continuum visco-plastic rheology for modelling the bath of small particles might be a promising approach in the future to clarify the origin of the segregation force.

Acknowledgements

This work was undertaken under the auspices of the ‘Laboratoire d’Excellence Mécanique et Complexité’ (ANR-11-LBX-0092), and ‘Initiative d’Excellence’ A*MIDEX (ANR-11-IDEX-0001-02). F.G. thanks I. Einav and B. Marks for fruitful discussions.

References

Aranson, I. S. & Tsimring, L. S. 2006 Patterns and collective behavior in granular media: theoretical concepts. *Rev. Mod. Phys.* **78**, 641–692.

Brey, J. J., Ruiz-Montero, M. J. & Moreno, F. 2005 Energy partition and segregation for an intruder in a vibrated granular system under gravity. *Phys. Rev. Lett.* **95**, 098001.

Da Cruz, F., Emam, S., Prochnow, M., Roux, J.-N. L. & Chevoir, F. 2005 Rheophysics of dense granular materials: discrete simulation of plane shear flows. *Phys. Rev.* E **72** (2), 021309.

Fan, Y. & Hill, K. M. 2011 Phase transitions in shear-induced segregation of granular materials. *Phys. Rev. Lett.* **106** (21), 218301.

https://doi.org/10.1017/jfm.2016.605 Published online by Cambridge University Press

FAN, Y. & HILL, K. M. 2015 Shear-induced segregation of particles by material density. *Phys. Rev.* E **92** (2), 022211.

FÉLIX, G. & THOMAS, N. 2004*a* Evidence of two effects in the size segregation process in dry granular media. *Phys. Rev.* E **70**, 051307.

FÉLIX, G. & THOMAS, N. 2004*b* Relation between dry granular flow regimes and morphology of deposits: formation of levées in pyroclastic deposits. *Earth Planet. Sci. Lett.* **221** (1–4), 197–213.

GUAZZELLI, E. & MORRIS, J. F. 2011 *A Physical Introduction To Suspension Dynamics*. Cambridge University Press.

GUILLARD, F., FORTERRE, Y. & POULIQUEN, O. 2014 Lift forces in granular media. *Phys. Fluids* **26** (4), 043301.

HILL, K. M., CAPRIHAN, A. & KAKALIOS, J. 1997 Axial segregation of granular media rotated in a drum mixer: pattern evolution. *Phys. Rev.* E **56**, 4386–4393.

JENKINS, J. T. & MANCINI, F. 1989 Kinetic theory for binary mixtures of smooth, nearly elastic spheres. *Phys. Fluids* A **1** (12), 2050–2057.

KLOSS, C., GONIVA, C., HAGER, A., AMBERGER, S. & PIRKER, S. 2012 Models, algorithms and validation for opensource DEM and CFD-DEM. *Prog. Comput. Fluid Dyn.* **12** (2), 140–152.

KOKELAAR, B. P., GRAHAM, R. L., GRAY, J. M. N. T. & VALLANCE, J. W. 2014 Fine-grained linings of leveed channels facilitate runout of granular flows. *Earth Planet. Sci. Lett.* **385**, 172–180.

MARKS, B., ROGNON, P. & EINAV, I. 2011 Grainsize dynamics of polydisperse granular segregation down inclined planes. *J. Fluid Mech.* **690** (2012), 499–511.

POULIQUEN, O., DELOUR, J. & SAVAGE, S. B. 1997 Fingering in granular flows. *Nature* **386** (6627), 816–817.

SAVAGE, S. B. & LUN, C. K. K. 1988 Particle size segregation in inclined chute flow of dry cohesionless granular solids. *J. Fluid Mech.* **189**, 311–335.

SCHLICK, C. P., FAN, Y., UMBANHOWAR, P. B., OTTINO, J. M. & LUEPTOW, R. M. 2015 Granular segregation in circular tumblers: theoretical model and scaling laws. *J. Fluid Mech.* **765**, 632–652.

THOMAS, N. 2000 Reverse and intermediate segregation of large beads in dry granular media. *Phys. Rev.* E **62** (1), 961–974.

THORNTON, A. R. & GRAY, J. M. N. T. 2008 Breaking size segregation waves and particle recirculation in granular avalanches. *J. Fluid Mech.* **596**, 261–284.

TRIPATHI, A. & KHAKHAR, D. V. 2011 Numerical simulation of the sedimentation of a sphere in a sheared granular fluid: a granular Stokes experiment. *Phys. Rev. Lett.* **107**, 108001.

WOODHOUSE, M. J., THORNTON, A. R., JOHNSON, C. G., KOKELAAR, B. P. & GRAY, J. M. N. T. 2012 Segregation-induced fingering instabilities in granular free-surface flows. *J. Fluid Mech.* **709**, 543–580.

https://doi.org/10.1017/jfm.2016.605 Published online by Cambridge University Press